

## Energy level schemes for far-infrared quantum well lasers

I. Lyubomirsky<sup>a)</sup> and Q. Hu

Department of Electrical Engineering and Computer Science and Research Laboratory of Electronics, Massachusetts Institute of Technology, Cambridge, Massachusetts 02139-4307

(Received 5 March 1998; accepted for publication 17 May 1998)

We analyze the physics of three-level and four-level systems for optically pumped far-infrared quantum well lasers. The higher complexity of the four-level system offers a great advantage because it gives more flexibility to design the dipole matrix elements and phonon scattering rates to enhance *both* the gain and emission efficiency. We propose a four-level scheme that is superior in gain and emission efficiency by an order of magnitude over previous designs. © 1998 American Institute of Physics. [S0003-6951(98)04029-7]

Lasers based on intersubband transitions in quantum wells were first proposed by Kazarinov and Suris in 1971.<sup>1</sup> An electrically pumped version of such a laser, called the Quantum Cascade Laser, was recently demonstrated by Faist *et al.*<sup>2</sup> The Quantum Cascade Laser operates by using a voltage bias to create a potential staircase in the conduction band with a quantum well forming each step. Electrons are injected from the contacts to cascade down the staircase. At each step the electrons emit photons in intersubband transitions from an excited state of the quantum well  $E_3$  to a lower state  $E_2$ . Electrons quickly vacate  $E_2$  via longitudinal optical (LO) phonon emission to the ground state  $E_1$ , which is also the excited state of the next step. This type of design has been very successful in covering the mid-infrared frequency range 4–11  $\mu\text{m}$ .<sup>3,4</sup> More recently, a mid-infrared quantum well laser operating at 15  $\mu\text{m}$  was realized by Gauthier-Lafaye *et al.* using optical pumping.<sup>5</sup> This laser also uses a simple three-level scheme, where electrons are optically pumped from the ground state  $E_1$  to the excited state  $E_3$ . A population inversion is ensured by designing the intersubband spacing  $E_2 - E_1 \sim 36$  meV for LO phonon resonance to quickly depopulate  $E_2$ . For longer wavelength lasers, optical pumping has the advantage of higher selectivity in populating energy levels while avoiding the free carrier losses associated with contact regions.

One may envision making an optically pumped far-infrared (FIR) quantum well laser by “scaling” the mid-infrared laser designs to longer wavelengths. Following this logical approach, several research groups have carried out optically pumped spontaneous emission experiments.<sup>6–8</sup> The measurement of FIR spontaneous emission from a quantum well laser structure is a crucial first step in the development of a laser. The strength of the emission or emission efficiency gives an indication of the design performance. The emission spectrum also provides a verification of the design emission frequency and linewidth. Unfortunately, the measurement of a clear FIR spontaneous emission spectrum has proven to be problematic. There are several experimental difficulties, like inherently low FIR emission efficiency, low collection efficiency, and sample heating, that may have contributed to the poor results. Another reason may be that pre-

vious designs have focused only on optimizing the gain.<sup>9,10</sup> Although the gain and emission efficiency are both proportional to the oscillator strengths of the pump and emission transitions, their dependence on phonon scattering rates is very different. In this letter, we propose a new quantum well design scheme that can be optimized using phonon engineering to enhance both the gain and emission efficiency.

To understand the difficulties involved in measuring optically pumped FIR spontaneous emission, we first analyze the simple three-level design. Figure 1 shows a prototype  $\text{Al}_{0.33}\text{Ga}_{0.67}\text{As}/\text{GaAs}$  coupled double well structure in analogy with the mid-infrared laser design.<sup>11</sup> The energy levels and wave functions are calculated numerically by solving Schroedinger and Poisson equations self-consistently.<sup>12</sup> Fermi’s Golden Rule is used to calculate phonon scattering rates, according to the method of Ferreira and Bastard.<sup>13</sup> All the calculations assume low temperature ( $\sim 4.2$  K) operation.

When a pump laser is tuned to the  $E_1 \rightarrow E_3$  transition, electrons are excited from the ground state  $E_1$  to level  $E_3$ . The steady state populations of levels  $E_1$ ,  $E_2$ , and  $E_3$  are determined by the fastest decay rates in the system. At low temperatures, LO phonon scattering leads to the fastest decay rate ( $\sim 1$  ps) for energy separations  $>36$  meV. Longitudinal

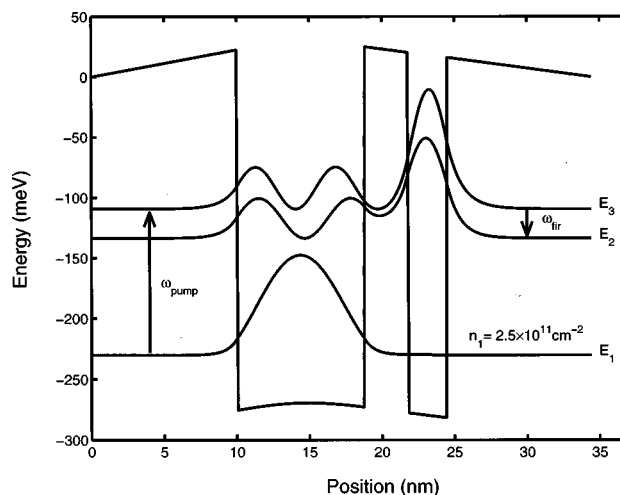


FIG. 1. Double quantum well structure for the three-level design scheme. The calculated transition energies are  $\Delta E_{31} = 120.7$  meV,  $\Delta E_{21} = 96.5$  meV, and  $\Delta E_{32} = 24.2$  meV. The calculated dipole matrix elements are  $Z_{21} = 17.6$  Å,  $Z_{32} = 43.4$  Å, and  $Z_{31} = 9.9$  Å.

<sup>a)</sup>Electronic mail: ilja@athena.mit.edu

acoustic phonon scattering gives the fastest decay rate ( $\sim 100$  ps) for FIR transitions  $< 36$  meV. The lasing transition  $E_3 \rightarrow E_2$  is designed such that  $E_3 - E_2 < 36$  meV to ensure a population inversion  $\Delta n = (1 - \tau_{21}/\tau_{32})n_3$ . The FIR spontaneous emission efficiency is given by

$$\eta_{3L} = \sigma_{31} n_1 \frac{\omega_{32}}{\omega_{31}} \frac{\tau_3^{\text{tot}}}{\tau_{32}^{\text{rad}}} \quad (1)$$

where  $\sigma_{31}$  is the cross section for absorption of a pump photon by an electron making transitions from  $E_1 \rightarrow E_3$ ,  $n_1$  is the ground state two-dimensional (2D) electron density,  $1/\tau_3^{\text{tot}}$  is the total nonradiative decay rate from level  $E_3$ , and  $1/\tau_{32}^{\text{rad}}$  is the spontaneous emission rate for the  $E_3 \rightarrow E_2$  transition. The spontaneous emission rate has an  $\omega_{32}^3$  dependence. Including the Manley–Rowe factor, the emission efficiency  $\eta_{3L}$  has an  $\omega_{32}^4$  dependence. Because of this unfavorable scaling factor, the FIR emission efficiency is many orders of magnitude lower than in the mid-infrared. For example, in the three-level quantum well design of Fig. 1,  $\sigma_{31} = 1.1 \times 10^{-14} \text{ cm}^2$ ,  $n_1 = 2.5 \times 10^{11} \text{ cm}^{-2}$ ,  $\omega_{32}/\omega_{31} = 0.20$ ,  $\tau_3^{\text{tot}} = 1.9$  ps, and  $\tau_{32}^{\text{rad}} = 2.8 \mu\text{s}$ , yielding a single well emission efficiency of  $3.6 \times 10^{-10}$ . In practice, the total efficiency is much lower because of poor FIR collection efficiency.<sup>6</sup>

It is difficult to see how  $\eta_{3L}$  can be improved by modifying the design of the three-level system. Increasing the doping density to increase  $n_1$  is not a good option because of free carrier absorption.<sup>5,14</sup> Increasing the dipole matrix element  $Z_{31}$  to increase the pump absorption cross section  $\sigma_{31}$  also does not work. The resulting stronger overlap between wave functions in levels  $E_1$  and  $E_3$  leads to a faster LO phonon scattering rate  $1/\tau_{31}$ . It is also difficult to increase the Manley–Rowe factor  $\omega_{32}/\omega_{31}$  because the only practical pump source (a CO<sub>2</sub> laser) operates in a narrow frequency range  $\sim 110\text{--}135$  meV. The only option available is to increase the number of quantum well periods. However, current molecular beam epitaxy (MBE) technology limits the number of periods ( $\sim 100$ ) to maintain uniformity.

Here is where the power of the quantum well as an ‘‘artificial atom’’ comes to our rescue. With quantum wells we have the ability to design wave functions and phonon scattering rates.<sup>15</sup> However, the simple three-level scheme does not give us enough flexibility to take advantage of this power. We will now show that increasing the complexity of our design by going to a four-level scheme will greatly improve our flexibility to design a larger emission efficiency. Let us consider the prototype four-level system shown in Fig. 2. This design employs three coupled quantum wells. The widths of the wells basically determine the energy levels, while the barrier widths determine the dipole matrix elements and to some extent the phonon scattering rates. Electrons are optically pumped from the ground state  $E_1$  to  $E_4$ .  $E_4 - E_3$  is separated by approximately one LO phonon energy (36 meV) so that electrons quickly decay from  $E_4$  to  $E_3$ . The laser emission occurs between levels  $E_3$  and  $E_2$  at  $\hbar\omega_{32} \sim 25$  meV. Electrons quickly decay from  $E_2$  to the ground state because  $E_2 - E_1 > 36$  meV. The spontaneous emission efficiency of the four-level system is given by

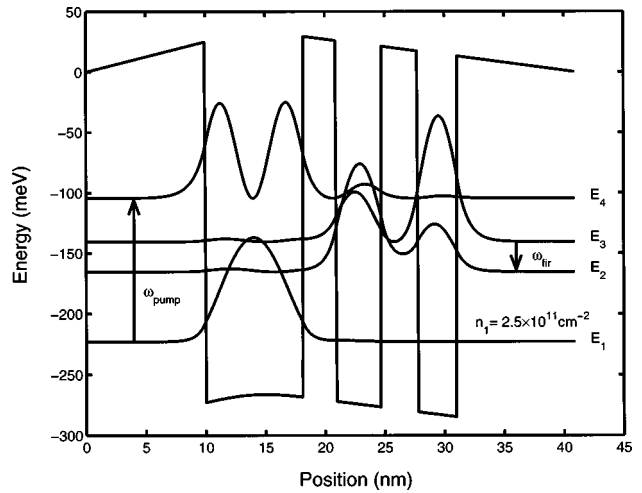


FIG. 2. Triple quantum well structure for the four-level design scheme. The calculated transition energies are  $\Delta E_{41} = 118.5$  meV,  $\Delta E_{31} = 82.4$  meV,  $\Delta E_{21} = 57.4$  meV, and  $\Delta E_{32} = 25.0$  meV. The calculated dipole matrix elements are  $Z_{21} = 9.7 \text{ \AA}$ ,  $Z_{32} = 32.0 \text{ \AA}$ ,  $Z_{31} = 6.1 \text{ \AA}$ ,  $Z_{41} = 18.6 \text{ \AA}$ ,  $Z_{43} = 23.6 \text{ \AA}$ , and  $Z_{42} = 11.0 \text{ \AA}$ .

$$\eta_{4L} = \sigma_{41} n_1 \frac{\omega_{32}}{\omega_{41}} \frac{\tau_4^{\text{tot}}}{\tau_{43}} \frac{\tau_3^{\text{tot}}}{\tau_{32}^{\text{rad}}} \quad (2)$$

At first sight it looks like this result is worse than the three-level case because of the extra ratio  $\tau_4^{\text{tot}}/\tau_{43}$ . Actually it is this extra ratio that allows us to bypass a major deficiency of the three-level design. We have designed the scattering rates such that  $1/\tau_{43}$  is the dominant contribution to  $1/\tau_4^{\text{tot}}$  so that  $\tau_4^{\text{tot}}/\tau_{43} \sim 1$ . Thus the absorption of the pump  $\sigma_{41}n_1$  is effectively decoupled from the LO phonon scattering rate  $1/\tau_3^{\text{tot}}$ . We can increase the dipole matrix element  $Z_{41}$  to increase  $\sigma_{41} \propto Z_{41}^2$  without effecting  $1/\tau_3^{\text{tot}}$ . This gives us the extra flexibility to increase the emission efficiency over previous designs.

Figure 3 shows a calculation of the emission efficiency as a function of electron density  $n_1$  for our design. For comparison, we have included the results of the three-level design. The four-level scheme gives an order of magnitude improvement at the electron density of  $\sim 2.5 \times 10^{11} \text{ cm}^{-2}$ . We also observe a resonance effect as the electron density is

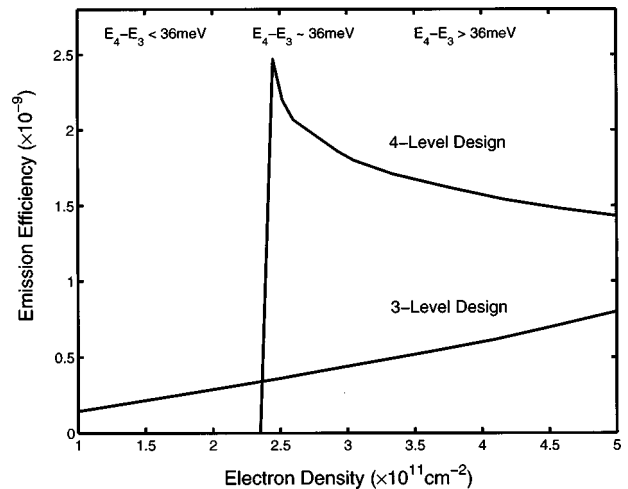


FIG. 3. Comparison of emission efficiency for the three-level and four-level designs.

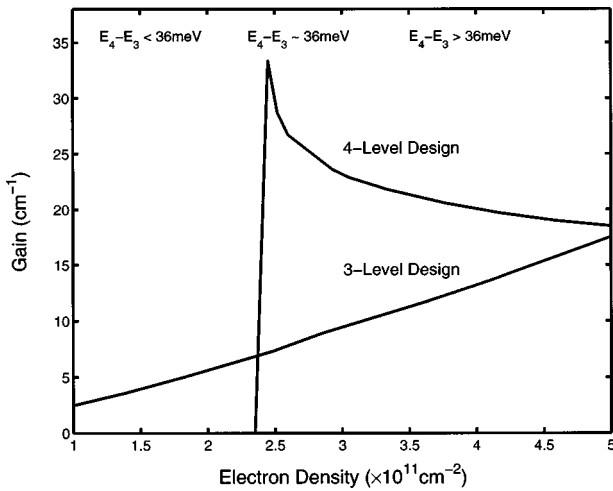


FIG. 4. Comparison of gain for the three-level and four-level designs.

varied and  $E_4 - E_3$  gets close to the LO phonon energy. The emission efficiency of the three-level scheme increases almost linearly with  $n_1$  and starts to catch up with  $\eta_{4L}$  at higher electron densities. Of course one can always design the optimum alignment  $E_4 - E_3 \sim 36$  meV to occur at higher electron densities, although operating at higher densities also increases the losses due to free carrier absorption.<sup>5</sup>

The same physics that allows us to improve spontaneous emission also leads to larger population inversion and gain. For small pump powers ( $\sim 1$  W), the population inversion is approximated by

$$\Delta n_{32} = \left[ \frac{\tau_3^{\text{tot}}}{\tau_{43}} \left( 1 - \frac{\tau_{21}}{\tau_{32}} \right) \frac{\tau_{21}}{\tau_{42}} \right] \frac{\tau_4^{\text{tot}}}{\tau_p} n_1, \quad (3)$$

where  $1/\tau_p = \sigma_{14} I_p / \hbar \omega_p$  is the pump rate of electrons from  $E_1 \rightarrow E_4$ . We have designed the phonon scattering rates such that  $\tau_3^{\text{tot}}/\tau_{43} \gg \tau_{21}/\tau_{42}$ ,  $\tau_3^{\text{tot}} \tau_{21}/\tau_{43} \tau_{32}$ , and  $\tau_4^{\text{tot}}/\tau_{43} \sim 1$ , so that  $\Delta n_{32} \approx n_1 \tau_3^{\text{tot}}/\tau_p$ . As in the design of the emission efficiency, we can now make  $\tau_3^{\text{tot}}$  as long as possible to increase the population inversion. Figure 4 shows the calculated gain for 1 W of cw pump power and 6 meV linewidth. The confinement factor is calculated assuming a slab waveguide geometry with metallic confinement.<sup>16</sup> The active region is composed of 100 quantum well periods separated by 200 Å barriers. The gain of the four-level design scheme is an order of magnitude larger than the three-level design at low electron densities.

The four-level scheme we proposed is not the only pos-

sibility. An alternative four-level design scheme would make the lasing transition  $E_4 \rightarrow E_3$  while designing the energy levels  $E_3 - E_2 \sim E_2 - E_1 \sim 36$  meV for enhanced depopulation of  $E_3$  via 2 LO phonon emission. This type of design was analyzed previously and found to have superior high temperature gain performance over an equivalent three-level design.<sup>10</sup> However, in terms of emission efficiency, this is basically a three-level system with a faster  $1/\tau_2^{\text{tot}}$  and  $1/\tau_3^{\text{tot}}$ . Therefore the emission efficiency is even worse than in a pure three-level system.

In conclusion, we have shown that scaling the mid-infrared three-level quantum well laser designs to longer wavelengths is not the best approach. The power of the quantum well as an ‘‘artificial atom’’ is evident in more complex design structures. We proposed a new four-level design scheme that takes advantage of our ability to design the dipole matrix elements and phonon scattering rates in a quantum well. The four-level scheme improves the emission efficiency and gain by an order of magnitude over previous designs. Although we focused our analysis on the optically pumped laser, these results may also prove useful for the electrically pumped case.

This work was supported by the U. S. Army Research Office under Grant Nos. DAAG55-97-1-0257 and DAAH04-95-1-0610.

- <sup>1</sup>R. F. Kazarinov and R. A. Suris, *Sov. Phys. Semicond.* **5**, 172 (1971).
- <sup>2</sup>J. Faist, F. Capasso, D. L. Sivco, C. Sirtori, A. L. Hutchinson, and A. Y. Cho, *Science* **264**, 553 (1994).
- <sup>3</sup>J. Faist, F. Capasso, D. L. Sivco, C. Sirtori, J. N. Baillargeon, A. L. Hutchinson, S.-N. G. Chu, and A. Y. Cho, *Appl. Phys. Lett.* **68**, 3680 (1996).
- <sup>4</sup>C. Sirtori, J. Faist, F. Capasso, D. L. Sivco, A. L. Hutchinson, and A. Y. Cho, *Appl. Phys. Lett.* **69**, 2810 (1996).
- <sup>5</sup>O. Gauthier-Lafaye, P. Boucaud, F. H. Julien, S. Sauvage, S. Cabaret, J. M. Lourtioz, V. Thierry-Mieg, and R. Planel, *Appl. Phys. Lett.* **71**, 3619 (1997).
- <sup>6</sup>J. W. Bales, Ph.D. thesis, Massachusetts Institute of Technology, 1991.
- <sup>7</sup>I. Lyubomirsky and Q. Hu, Oral Presentation, MRS Fall Meeting (1997).
- <sup>8</sup>J. Faist (private communications, 1997).
- <sup>9</sup>V. Berger, *Semicond. Sci. Technol.* **9**, 1493 (1994).
- <sup>10</sup>P. Harrison and R. W. Kelsall, *J. Appl. Phys.* **81**, 7135 (1997).
- <sup>11</sup>F. H. Julien, A. Sa’ar, J. Wang, and J. P. Leburton, *Electron. Lett.* **11**, 838 (1995).
- <sup>12</sup>Band nonparabolicity is handled using the method of D. F. Nelson, R. C. Miller, and D. A. Kleinman, *Phys. Rev. B* **35**, 7770 (1987).
- <sup>13</sup>R. Ferreira and G. Bastard, *Phys. Rev. B* **40**, 1074 (1989).
- <sup>14</sup>H. N. Spector, *Phys. Rev. B* **28**, 971 (1983).
- <sup>15</sup>I. Lyubomirsky, B. Xu, and Q. Hu, *LEOS Newsletter* **11**, 13 (1997).
- <sup>16</sup>B. Xu, Q. Hu, and M. R. Melloch, *Appl. Phys. Lett.* **70**, 2511 (1997).